Stochastic procedures for extreme wave induced responses in flexible ships

Jensen, Jørgen Juncher; Andersen, Ingrid Marie Vincent; Seng, Sopheak

Published in:
International Journal of Naval Architecture and Ocean Engineering

Link to article, DOI:
10.2478/IJNAOE-2013-0236

Publication date:
2014

Document Version
Publisher's PDF, also known as Version of record

IJNAOE
©SNAK, 2014

Int. J. Nav. Archit. Ocean Eng. (2014) 6:1148~1159
http://dx.doi.org/10.2478/IJNAOE-2013-0236
pISSN: 2092-6782, eISSN: 2092-6790

Stochastic procedures for extreme wave induced responses in flexible ships

Jørgen Juncher Jensen, Ingrid Marie Vincent Andersen and Sopheak Seng

Department of Mechanical Engineering, Technical University of Denmark, DK 2800, Denmark

ABSTRACT: *Different procedures for estimation of the extreme global wave hydroelastic responses in ships are discussed. Firstly, stochastic procedures for application in detailed numerical studies (CFD) are outlined. The use of the First Order Reliability Method (FORM) to generate critical wave episodes of short duration, less than 1 minute, with prescribed probability content is discussed for use in extreme response predictions including hydroelastic behaviour and slamming load events. The possibility of combining FORM results with Monte Carlo simulations is discussed for faster but still very accurate estimation of extreme responses. Secondly, stochastic procedures using measured time series of responses as input are considered. The Peak-over-Threshold procedure and the Weibull fitting are applied and discussed for the extreme value predictions including possible corrections for clustering effects.*

KEY WORDS: Extreme value predictions; Stochastic processes; First order reliability method (FORM), Peak-over-threshold, Monte carlo simulations.

INTRODUCTION

With the increasing size of container ships due account should be made to possible hydroelastic contributions to the hull girder response from the waves. This was the background for the TULCS project ('Tools for Ultra Large Container Ships', EU Grant no. 234146) with the objective "The final goal is to deliver clearly validated design tools and guidelines, capable of analyzing all hydro-structure interaction problems relevant to Ultra Large Container Ships". In the project two main areas were the development of advanced hydrodynamic calculation procedures and the analysis of extensive full scale measurements onboard the TULCS case vessel. Both local and global hydro-elastic responses were considered as well as consequences in terms of higher extreme values and increased expected fatigue damage. The outcome of the TULCS project has been presented in numerous papers and an overall description can be found in the paper, Malenica and Derbanne (2012), by the project coordinators.

The present paper deals with stochastic procedures applied in the TULCS project to the hydro-elastic global responses in order to estimate proper extreme responses. Two procedures are considered.

The first procedure deals with the problem faced using advanced CPU demanding hydrodynamic CFD calculation procedures. Here stochastic simulations using random wave sequences become prohibited expensive if events with large return periods are considered. The suggested solution is based on the theory of conditional processes where critical wave episodes are derived with prescribed probability content using the First Order Reliability Method (FORM) coupled with Monte Carlo Si-

Corresponding author: *Jørgen Juncher Jensen*, e-mail: *jjj@mek.dtu.dk*

mulations. Thereafter, a Modal Correction Factor is used to map the responses from the less expensive non-linear hydrodynamic code used in the FORM analysis to the outcome of the CFD calculations performed using the same critical wave episodes. An example for the TULCS case vessel is given.

The second procedure looks at the full-scale strain measurements taken in the hull girder. Different methods, a Weibull model of the individual peak value distribution, a Peak-over-Threshold model looking at the tail behavior, only, and the ACER procedure, Naess and Gaidai (2009), accounting for clustering effects have been applied. A comparison in terms of the derived Gumbel distributions for the three hours maximum wave-induced bending moment for the different procedures is shown for a specific extreme measured case.

The procedures considered have proven rather effective in the cases considered, but general conclusions regarding accuracy cannot be given.

DEFINITION OF CRITICAL WAVE EPISODES FOR CFD CALCULATIONS

First Order Reliability Method (FORM) for stationary processes

The excitation or input process is considered to be a stationary stochastic process. The input process is the wave elevation and the associated wave kinematics.

For moderate sea states the wave elevation can be considered as Gaussian distributed, whereas for more severe sea states non-linearities in the wave model must be incorporated. A second-order stochastic wave model was used in Jensen and Capul (2006) and can easily be included as it does not involve additional stochastic parameters. Linear, long-crested waves are thus the basic input process. Hence, the normal distributed wave elevation $H(x,t)$ as a function of space x and time t can be written in discretized form as

$$H(x,t) = \sum_{i=1}^{n} \left(u_i c_i(x,t) + \overline{u}_i \overline{c}_i(x,t) \right) \tag{1}$$

where the variables $u_i, \overline{u}_i$ are statistically independent, standard normal distributed variables and with the deterministic coefficients given by

$$\begin{aligned} c_i(x,t) &= \sigma_i \cos(\omega_i t - k_i x) \\ \overline{c}_i(x,t) &= -\sigma_i \sin(\omega_i t - k_i x) \\ \sigma_i^2 &= S(\omega_i)\Delta\omega_i \end{aligned} \tag{2}$$

where $\omega_i, k_i = \omega_i^2 / g$ are the n discrete frequencies and wave numbers applied. Here g is the acceleration of gravity. Furthermore, $S(\omega)$ is the wave spectrum and $\Delta\omega_i$ the increment between the m discrete frequencies applied. From the wave model, Eqs. (1)-(2), and the associated kinematics any non-linear wave-induced response $\phi(t)$ can in principle be determined by a time domain analysis using a proper hydrodynamic model including e.g. also second order wave components:

$$\phi = \phi(t \,|\, u_1, \overline{u}_1, u_2, \overline{u}_2, \ldots, u_n, \overline{u}_n) \tag{3}$$

Each of these realisations represents the response for a possible wave scenario. The realisation which exceeds a given threshold ϕ_0 at time $t=t_0$ with the highest probability is sought. This problem can be formulated as a limit state problem, well-known within time-invariant reliability theory, Der Kiureghian (2000):

$$G(u_1, \overline{u}_1, u_2, \overline{u}_2, \ldots, u_n, \overline{u}_n) \equiv \phi_0 - \phi(t_0 \,|\, u_1, \overline{u}_1, u_2, \overline{u}_2, \ldots, u_n, \overline{u}_n) = 0 \tag{4}$$

An approximate solution can be obtained by use of First Order Reliability Methods (FORM). The limit state surface G is given in terms of the statistically independent standard normal distributed variables $\{u_i, \overline{u}_i\}$ and determination of the design point, $\{u_i^*, \overline{u}_i^*\}$, defined as the point on the failure surface, $G = 0$, with the shortest distance to the origin of $\{u_i, \overline{u}_i\}$, is rather straightforward, Der Kiureghian (2000). A linearization around this point replaces Eq. (4) with a hyper plane in $2n$ space. The distance, β_{FORM}, from the hyper plane to the origin is denoted the (FORM) reliability index and is equal to

$$\beta_{FORM} = -\Phi^{-1}\left(\phi(t_0 \,|u_1, \overline{u}_1, u_2, \overline{u}_2, ..., u_n, \overline{u}_n) > \phi_0 \,|\text{FORM linearization}\right) \tag{5}$$

where Φ^{-1} is the inverse standard normal distribution function. Thus the reliability index directly relates to the probability of exceedance. The calculation of the design point $\{u_i^*, \overline{u}_i^*\}$ and the associated value of β_{FORM} can be performed by standard reliability codes, e.g. Det Norske Veritas (2002), or by standard optimization codes (i.e. minimizing the distance β with the constraint Eq. (4)) in which $\phi(t_0)$ has to be calculated by numerical integration for a number of combinations of $\{u_i, \overline{u}_i\}$ until the design point is reached. The integration must cover a sufficient long time period $\{0,t_0\}$ to avoid any influence on $\phi(t_0)$ of the initial conditions at $t=0$, i.e. to be longer than the memory in the system. As no explicit expression for $\phi(t_0)$ is needed, any kind of non-linearities can be incorporated including e.g. impact loads due to slamming. Note that the reliability procedure only gets $\phi(t_0)$ as input and no information about the time evolution leading to $\phi(t_0)$.

Proper values of t_0 would usually be 50-300 *seconds*, depending on the damping in the response considered. Hence, to avoid repetition in the wave system and for representation of typical wave spectra n = 10-50 would be needed.

Mean out-crossing rates and peak value distribution

The time-invariant peak distribution of the responses is of main interest for design. Extreme values in stationary stochastic processes are usually dealt with either by the Poisson model or order statistics. In both cases the basic parameter is the mean out-crossing rate. For upward unbounded responses R, both models lead to the Gumbel distribution for the asymptotic extreme response, e.g. Jensen (2009):

$$\begin{aligned} &\text{Order statistics } \rightarrow \text{Poisson up-crossings:} \\ &P(\max(R) < \phi_0 \,|0 < t < T) = F_p^N(\phi_0) = \left(1 - \frac{\nu(\phi_0)}{\nu(0)}\right)^N = \left(1 - \frac{T\nu(\phi_0)}{N}\right)^N \underset{N\to\infty}{\rightarrow} \exp\left(-T\nu(\phi_0)\right) \end{aligned} \tag{6}$$

where T and $N = \nu(0)T$ are the total time and number of peaks, respectively, and $F_p(\phi_0)$ the cumulative density function of the peaks of ϕ_0. Generally, the Poisson model is accurate for high threshold levels except for very narrow banded or multi-modal responses. In such cases, VanMarcke's first-passage probability, VanMarcke (1975), can be used with spectral moments depending on the threshold ϕ_0, see Fujimura and Der Kiureghian (2007) and Garrè and Der Kiureghian (2010).

Within a FORM approximation the mean out-crossing rate $\nu(\phi_0)$ can be written, Jensen and Capul (2006)

$$\begin{aligned} &\nu(\phi_0) = \frac{1}{2\pi}\exp\left(-\frac{1}{2}\beta_{FORM}^2\right)\sqrt{\sum_{i=1}^{n}\left(\alpha_i^2 + \overline{\alpha}_i^2\right)\omega_i^2} \equiv \nu_0(\phi_0)\exp\left(-\frac{1}{2}\beta_{FORM}^2\right) \\ &\{\alpha_i, \overline{\alpha}_i\} = \frac{\{u_i^*, \overline{u}_i^*\}}{\beta_{FORM}} \end{aligned} \tag{7}$$

Thus the mean out-crossing rate can be expressed analytically in terms of the design point and the reliability index. For linear processes $\beta_{FORM} = \phi_0 / s_\phi$, where s_ϕ is the standard deviation of the response ϕ and Eq. (7) becomes the Rayleigh distribution.

Design wave episodes

When the design point has been determined, a critical wave episode can be defined by Eqs. (1)-(2) with $\{u_i, \overline{u}_i\} = \{u_i^*, \overline{u}_i^*\}$. This critical or most probably episode can be considered as a design episode and could be used as input in e.g. model tests or full non-linear deterministic CFD response calculations, Seng et al. (2012) and Seng and Jensen (2013), using e.g. a non-linear strip theory procedure in Eq. (3) for generation of the design episode, Andersen and Jensen (2012). An example is shown below.

The increasing size of container vessels give rise to structural issues in ship design. The very long container vessels (up to 400 *m* in length) become structurally "softer" with increasing length which means that their natural hull vibration frequencies will be significantly reduced. The EU project Tools for Ultra Large Container Ships (TULCS) addresses these issues related to very large container ships such as the TULCS case ship. A non-linear strip theory analysis is carried out for this vessel, Andersen and Jensen (2012), comparing the rigid and flexible modelling of the case ship using a specified maximum vertical bending moment amidships in both sagging and hogging. The specified maximum bending moment is less than the maximum bending moment stated by the class rules and is thus not necessarily related to the more severe sea states, and no green water on deck occurs. Transient, linear conditional waves representing the most probable wave scenario are determined by the FORM approach.

The most probable conditional wave scenario that will cause a vertical bending moment of 5 *GNm* in sagging condition (negative bending moment) for the flexible ship is shown in Fig. 1(a). The illustrated wave is the encounter wave as seen from amidships. The corresponding vertical bending moment for the flexible and the rigid ship is shown in Fig. 1(b). The effect of the hull flexibility is clearly seen and it can be observed that the hull becomes elastically excited (whipping) just after t = 50 *sec*. as a result of a slamming event. In the same figure the vertical bending moment is illustrated for the rigid ship using the same conditional wave as for the flexible ship in order to illustrate the effect of hull flexibility. It is observed that the hull flexibility increases the amplitudes of the subsequent peaks in the bending moment.

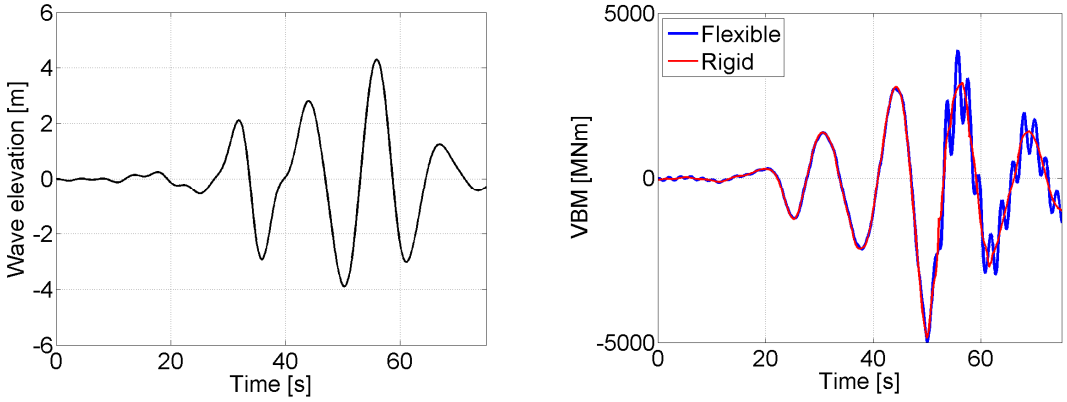

(a) The incoming waves amidships. (b) The vertical wave-induced bending moment.

Fig. 1 The conditional wave and corresponding vertical wave bending moment conditioned on a vertical bending moment of 5,000 *MNm* at 50 *sec.* in sagging condition.

In order to judge the important of these approximations a full CFD calculation has been done in Seng and Jensen (2013) with the same conditional wave as input. The free surface method applied in the study is based on the single phase incompressible Navier-Stokes solver provided as a standard solver in the open source CFD toolbox OpenFOAM. The free surface is captured using a single fluid Volume of Fluid (VOF) formulation solving the incompressible Navier-Stokes equation with the effective fluid density and viscosity evaluated from a weighting using the phase-fraction function. For details see also Seng et al. (2012). The hull girder is allowed to deform according to the Timoshenko beam solution which is integrated with the fluid solver in a fully coupled two-way partitioned scheme.

Under the same wave sequence as applied in the nonlinear time-domain strip theory (see Figs. 1(a)) , the time series of VBM predicted by the free surface CFD method is shown as the thick line in Fig. 2 whereas the flexible ship result from Fig. 1(b) is redrawn as the thin line. The wave sequence was targeting a VBM amidships at 5,000 *MNm* using the non-linear strip

theory as hydrodynamic model, but according to the CFD result the peak value is only 3,878 *MNm* as evaluated from the peak sagging response around the target time $t = 50$ *sec.* In both cases the structural model was the same Timoshenko beam model.

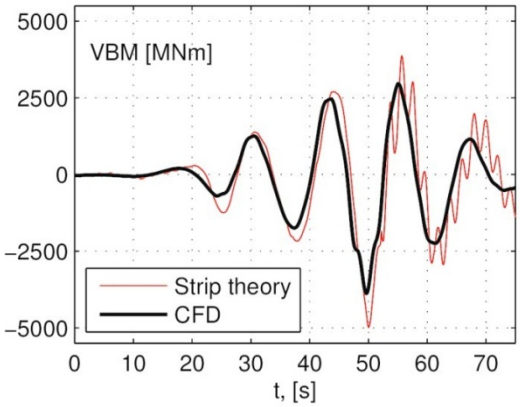

Fig. 2 The vertical wave bending moment conditioned on a vertical bending moment of 5,000 *MNm* at 50 *sec.* In sagging condition. The conditional wave used in CFD is the one obtained using strip theory.

Obviously the CFD calculation changes the result quite significantly and a detailed investigation of the reasons for the differences is given in Seng and Jensen (2013). It was found that the non-linear strip theory estimates the most probably wave scenario to be the one where slamming occurs in the aft part of the vessel on the large flat overhang above the propeller. This happens when the wave induced sagging condition is close to its maximum value and therefore no whipping vibrations are seen before $t = 50$ *sec.* In the non-linear strip theory the hydrodynamic coefficients are determined at the instantaneous free surface of the incident wave, taking into account the heave and pitch of the vessel. This produce an impulse-like force in the aft part of the vessel at the instant where the dry stern becomes wet, i.e. at $t = 49$-51 *sec.* No significant slamming is seen in the forward part of the vessel. From the CFD calculation using the same wave scenario it appears that this stern slamming event does not appear as the stern is wet all the times due to the modification of the incident wave by the wave diffraction from the hull. Thus in this case the non-linear strip theory is not a good predictor of what will be the most probable wave scenario leading to a given response. Further studies are needed to resolve this problem. It should, however, be emphasized that the non-linear strip theory usually captures reasonably well the physics of low frequency wave-induced responses, i.e. rigid body hydrodynamics, resulting in good agreement with CFD calculations, c.f. Seng et al. (2012).

Monte carlo simulations

To improve the accuracy of the FORM results additional Monte Carlo Simulations (MCS) can be performed. In order to increase the mean out-crossing rate and thereby reduce the simulation time in the MCS calculations, the wave elevation *S(ω)* spectra can be multiplied by a factor γ^2. From the FORM analysis it is known that this will just change the reliability index β_{FORM} by a factor $1/\gamma$, Jensen (2007), Fujimura and Der Kiureghian (2007), Garrè and Der Kiureghian (2010) and Jensen (2011). As the FORM result is asymptotically exact for small out-crossing rates, i.e. for large values of β_{FORM} and thereby small values of γ, it is expected that the MCS results for the reliability index as function of the load intensity could be approximated accurately by

$$\beta_{MCS} = \beta_{FORM} + a\gamma^b \tag{8}$$

The coefficients a and b (≥ 0) can be determined from two MCS calculations using values of γ sufficient larger than one to ensure reasonable calculation times for the MCS calculations. The validity of this hypothesis has been proved in Jensen (2011) for two examples. The design or actual value β_{actual} for the reliability index is finally obtained by taking $\gamma = 1$ in Eq. (8) with the corresponding exceedance probability

$$P(\max(R) > \phi_0 \,|\, 0 < t < T) = 1 - \exp\left(-T\nu(\phi_0)\right) = 1 - \exp\left[-\nu_0 T \exp\left(-0.5\beta\left(\phi_0\right)^2_{actual}\right)\right] \tag{9}$$

according to Eq. (6). Here ν_0 is the zero mean out-crossing rate to be estimated from a time signal of the response or from the FORM result, Eq. (7),

$$\nu_0(\phi_0) = \frac{1}{2\pi}\sqrt{\sum_{i=1}^{n}\left(\alpha_i^2 + \overline{\alpha}_i^2\right)\omega_i^2} \tag{10}$$

Note that ν_0 in Eq. (10) depends on the threshold level ϕ_0, but usually this dependence is small except for very small threshold levels.

If only MCS calculations are performed one can of course also make use of the $1/\gamma$ dependence of the FORM reliability index with load intensity. Hence, Eq. (8) could be replaced by

$$\beta_{MCS} = \frac{c}{\gamma} + a\gamma^b \tag{11}$$

The coefficients *a*, *b* and *c* must be determined by three MCS calculations using three values of γ, all greater than one. Often a linear fit, *b* = 0, is sufficient. However, without the FORM result the correct asymptotical behavior for $\gamma \to 0$ is not ensured.

If the probability distribution of the extreme response peaks ϕ_0 is needed rather than just the exceedance level of a specific value of ϕ_0 then the FORM procedure is less useful as it has to be redone for each new value of the threshold ϕ_0. However, the result, Eq. (11), can be obtained readily from a single set of MCS for any value of ϕ_0 with *a, b* and *c* being (numerical) functions of ϕ_0. The peak value distribution is still given by Eq. (9), using Eq. (11) with $\gamma = 1$.

Often the peak value distribution of the maximum peak among *N* peaks is formulated as a Gumbel distribution:

$$P(\max(R) < \phi_0 \,|\, N \ peaks) = \exp\left[-\exp\left(-\left(\phi_0 - \tilde{\phi}_N\right)/\hat{\phi}_N\right)\right] \tag{12}$$

Comparing Eq. (12) and Eq. (9) with $N = \nu_0 T$ shows that the Gumbel distribution is a linear approximation to the real distribution and that the best choice of coefficients $\tilde{\phi}_N, \hat{\phi}_N$ in the Gumbel distribution is given by:

$$\begin{aligned} &\beta(\tilde{\phi}_N) = \sqrt{2\ln(N)} \\ &\hat{\phi}_N = \frac{1}{\beta(\tilde{\phi}_N)\beta'(\tilde{\phi}_N)}; \quad \beta'(\tilde{\phi}_N) \equiv \left.\frac{d\beta(\phi_0)}{d\phi_0}\right|_{\phi_0=\tilde{\phi}_N} \end{aligned} \tag{13}$$

The MCS must thus be used to estimate the value of the threshold $\phi_0 = \tilde{\phi}_N$ yielding a reliability index $\beta = \sqrt{2\ln(N)}$, where the number of peaks $N = \nu_0 T$ depends on the duration *T* over which the extreme peak distribution is requested (e.g. minutes, hours or annually). Also the slope, $\beta'(\tilde{\phi}_N)$, at this threshold value must be estimated for use in Eq. (13). It can be noted that $\tilde{\phi}_N$ is very close to the most probable value of the maximum peak among *N* peaks provided *N* is large. Thereby $\beta = \sqrt{2\ln(N)}$ becomes directly associated with the most probable response among *N* peaks. For linear systems, where $\beta = \phi_0/\sigma_\phi$ with σ_ϕ being the standard deviation of the response, the well-known result $\tilde{\phi}_N = \sigma_\phi\sqrt{2\ln(N)}$ appears.

It should be noted, that if *N* is much smaller than the actual value relevant for design, the linearization in Eqs. (12)-(13) will result in an inaccurate estimate of the probability of exceedance of the design threshold value. This is the drawback in the use of the Gumbel (or Weibull) fitting procedure.

Finally, the long-term probability distribution is obtained as usual by weighting Eq. (9) or (12) with the joint probability density function of the sea state and operational parameters (e.g. significant wave height, mean period, ship speed etc.). This joint probability density function must normally be based on some approximations regarding the statistical dependencies between these parameters.

EXTREME VALUE PREDICTIONS BASED ON FULL SCALE MEASUREMENTS

Currently many new ships are equipped with sensors measuring various ship responses like accelerations and strains. These measurements can be used in operational decision support regarding expected maximum responses within the next couple of hours and also for verification/modification of current rule values used in design. The main result from the analysis of the measurements is the most probable extreme events within a given time T of the order hours together with its probability distribution. Generally, the Gumbel distribution is accepted as the proper extreme value distribution even if it is only asymptotically correct (and under the assumption of no upwards bounded response, which is unphysical in reality). A modification of the Gumbel distribution has been suggested by Naess and co-workers, e.g. Naess and Gaidai (2008) which includes an additional parameter able to model better distributions for moderate response levels. However, in the present discussion the Gumbel distribution is taken as the extreme value distribution, but modifications to use the Naess and Gaidai formulation instead is straightforward. The Gumbel distribution is a two parameter distribution and the task is then to determine these two parameters from the actual measurements.

Individual peak distribution

The first step in the derivation of the extreme value distribution is to analyze the individual peak value distribution, because from this distribution a Gumbel distribution of the extreme value distribution for the largest peak among N peaks can readily obtained. It follows from Eq. (6) that if the individual peak value distribution is of the form.

$$F_p(x) = 1 - \exp(-q(x)) \tag{14}$$

Then the most probable maximum value x_{mpl}, i.e. the value with a return probability of 1/N follows from $q\left(x_{mpl}\right) = \ln(N)$. The associated Gumbel distribution is then found by linearization around x_{mpl}:

$$\begin{aligned} &P(\max(R) < x \,|\, 0 < t < T) = F_p^N(x) = \left[1 - \exp(-q(x))\right]^N \\ &\underset{N\to\infty}{\rightarrow} \exp\left[-N\exp(-q(x))\right] \approx \exp\left[-\exp\left\{-q'(x_{mpl})\left(x - x_{mpl}\right)\right\}\right] \end{aligned} \tag{15}$$

with $q'(x) = dq(x)/dx$. The question is then the choice of individual peak value distribution. It is well-known that for a narrow-banded Gaussian process the individual peaks becomes Rayleigh distributed. In general broad-band and non-Gaussian effects will influence the peak distribution. However, for typical wave-induced responses like accelerations and strains/stresses the Weibull distribution:

$$F(x;a,b) = 1 - \exp\left(-\left(\frac{x}{a}\right)^b\right) \tag{16}$$

has been shown in numerous cases to be a very versatile and accurate model for measured peak distributions. An example is shown in Fig. 3 dealing with the same ship as in the previous examples. The curve denoted WF is the filtered signal removing hydroelastic contributions from the hull girder vibrations whereas the WF+HF curve is derived directly from the measured time signal.

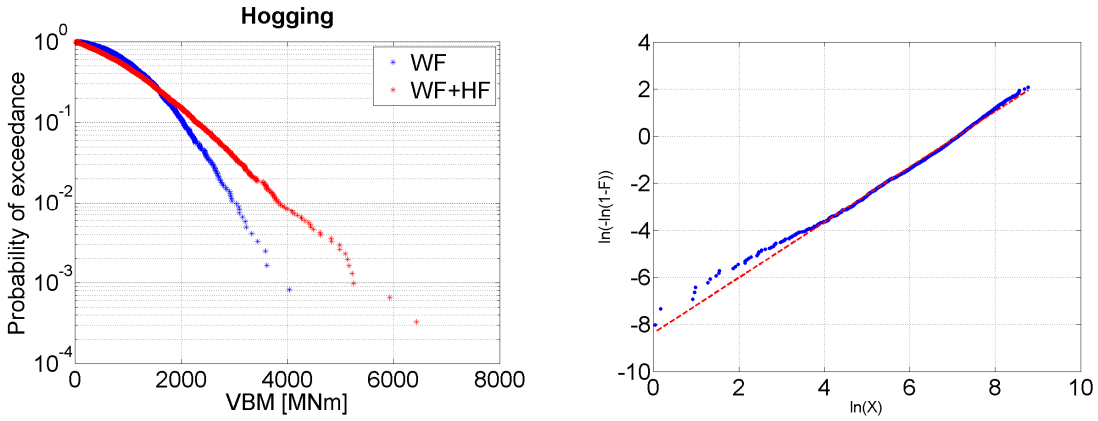

(a) Measured peak value distribution. (b) Weibull fit to the WF+HF curve.

Fig. 3 Individual peak value distribution for the hogging wave bending moment for a container ship taken from measurement over a time period of three hours.

Clearly a significant contribution from the hydroelastic deformation of the hull girder is visible in the wave-induced bending moment making the maximum value measured during three hours close to the design value (rule value). As shown in Andersen and Jensen (2014), the hydroelastic contribution is nearly solely in the form of the two node vertical vibration mode. The present analysis is focused on responses for flexible ships and hence this measured rather extreme three hours measurement is a good real test case for the stochastic prediction methods. Fig. 3(b) shows a Weibull fit of the WF+HF curve in Fig. 3(a). As the tail behavior is of main interest in the extreme value predictions, the Weibull seems a reasonable model here, but with some overestimation of the largest peaks. From the Weibull distribution, Eq. (16), the parameters in the Gumbel distribution, Eq. (15), become

$$x_{mpl} = a\sqrt[b]{\ln(N)}; \quad q'(x_{mpl}) = \frac{b}{a}\left[\ln(N)\right]^{1-1/b} \tag{17}$$

The Gumbel distribution for the three hours maximum wave bending moment for the case shown in Fig. 3(b) is shown in Fig. 4. The maximum measured value during the three hours is included in the figure and seen to be well below the most probable value, i.e. the value corresponding to the maximum value of the density function. The reason is that the Weibull fit in this case overestimate the tail distribution as mentioned above.

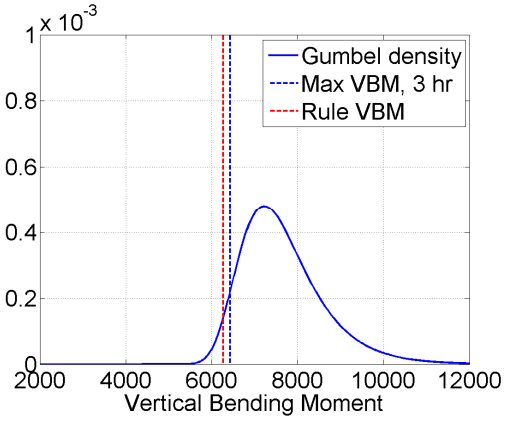

Fig. 4 Gumbel probability density function for the three hours maximum wave bending moment for the case shown in Fig. 3(b).

Peak-over-threshold

In order to focus on the largest measured peaks in the derivation of the Gumbel distribution the Peak-over–Threshold method can be a useful procedure. From the theoretical background for the method it is known that if the excess *x-u* over the threshold *u* is exponential distributed then the asymptotic extreme value distribution is the Gumbel distribution. The relations between the parameter *c* in the exponential distribution $F(x;c,u)=1-\exp(-(x-u)/c)$ and the Gumbel distribution are $x_{mpl}=u+c\ln(N_u)$; $q'(x_{mpl})=1/c$, where N_u is the number of peaks above the threshold *u*. The choice of threshold is somewhat arbitrary. A too high value will obviously limit the number of peaks used in the determination of the parameter *c*. A useful property of the method is that the mean value of the excess should be equal to the parameter *c* for Gumbel type of asymptotic extreme value distributions and not dependent on *u*. Thus a plot of the mean value of the excess for different value of *u* can be used to select a proper value of *u.* An example is shown in Fig. 5(a). Clearly some variation of the mean excess with threshold is seen, but if the threshold are chosen between 2,000 *GNm* and 4,000 *GNm* then the variation is not large.

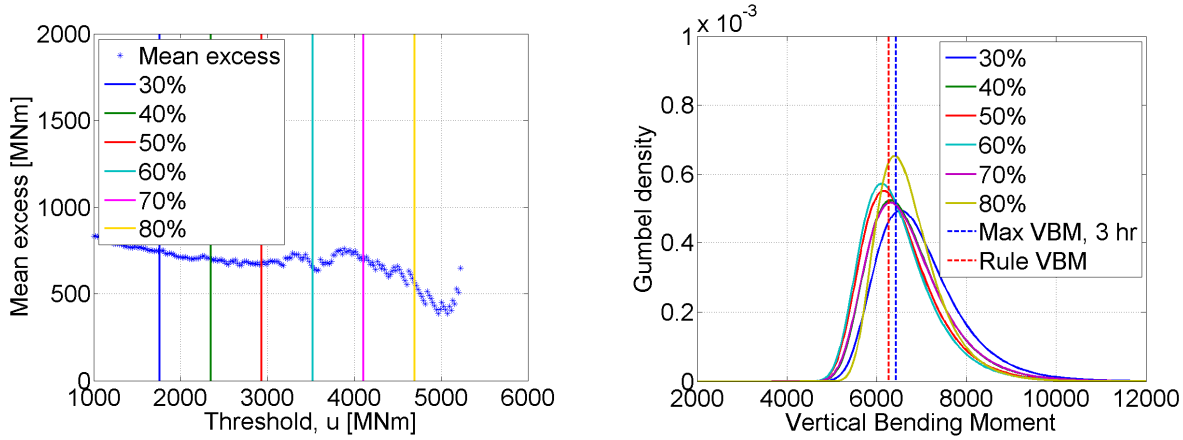

(a) Mean excess as function of threshold *u*. (b) Corresponding Gumbel distributions.

Fig. 5 Peak-over-threshold analysis for the three hours maximum wave bending moment for the case shown in Fig. 3(b). The percentage shown for the threshold is relative to maximum measured peak value

Based on the exponential fit to the excess, i.e. the parameter *c,* for different value of *u* the Gumbel distributions become as shown in Fig. 5(b). It is seen that the variation with threshold *u* is rather modest.

Comparing the Gumbel distribution derived from the Weibull fit in Fig. 4 with the ones in Fig. 5(b) from the Peak-over-Threshold method the latter are clearly more in agreement with the measurements as the most probable values in the Gumbel distributions now are quite close to the maximum measured peak value.

Clustering of peaks

Extreme value analysis based on Eq. (15) assumes independent peaks. Especially with hydroelastic responses occur due to impulse loads this is a questionable assumptions as large peaks then occur in clusters. Naess and co-workers, e.g. Naess and Gaidai (2009), have developed an efficient procedure for de-clustering a time signal. Here a short description is given focusing on just correlations between two adjacent peaks.

Consider the extreme value distribution for *N* peaks: $X_i; i=1,2,...,N$ in a measured stochastic process:

$$P(\max X_i \le x \,|\, i=1,2,..,N) = P(X_1 \le x, X_2 \le x, ..., X_N \le x) \tag{18}$$

The peaks are numbered according to the instant in time instant where measured. Assuming a large number *N* of peaks and large exceedance levels *x*, i.e. $P(X_i > x) << 1$ then for statistically independent peaks Eq. (18) can be written

$$P(\max X_i \le x | i = 1,2,...,N) \approx \exp(-N\varepsilon_1(x)) \tag{19}$$

where $\varepsilon_1(x) = \frac{1}{N}\sum_{i=1}^{N} P(X_i > x)$ can be considered as the mean up-crossing rate $\nu(x)/\nu(0)$ in accordance with Eq. (6). However, if two adjacent peaks are correlated then Eq. (18) reads

$$P(\max X_i \le x | i = 1,2,..,N) = P(X_1 \le x)\prod_{i=2}^{N} P(X_i \le x | X_{i-1} \le x) \tag{20}$$

Again, for large exceedance levels x $P(X_i > x) \approx 1$ and $\alpha_{2i}(x) = P(X_i > x | X_{i-1} \le x) << 1$. Hence, Eq. (20) can be re-written as:

$$P(\max X_i \le x | i = 1,2,..,N) \approx \prod_{i=2}^{N}(1-\alpha_{2i}(x)) \approx \exp\left(-N\varepsilon_2(x)\right) \tag{21}$$

where

$$\varepsilon_2(x) = \frac{1}{N-1}\sum_{i=2}^{N}\alpha_{2i}(x) \tag{22}$$

In the analysis of a given set of peaks $\alpha_{2i}(x)$ is most easily obtained by the indicator function:

$$\alpha_{2i}(x) = \begin{cases} 1 & \text{if } X_i > x \text{ and } X_{i-1} \le x \\ 0 & \text{otherwise} \end{cases} \quad ; \quad i = 1,2,..,N \tag{23}$$

Thus the extreme value formulation for correlated peaks, Eq. (22), has the same form as for uncorrelated peaks, Eq. (19), and hence $\varepsilon_2(x)$ can be considered as an average up-crossing rate accounting for clustering, denoted Average Conditional Exceedance Rate (ACER) in Naess and Gaidai (2009), where also derivations considering clustering between any number of adjacent peaks are given.

Fig. 6(a) shows ε_1 and ε_2 derived from the same measurements as used in the previous figures. Clearly clustering effects are important. This is also evident from Fig. 6(b) which shows a comparison between the Gumbel fit to these measurements using the procedures described here. The result included in Fig. 6(b) from the ACER procedure are obtained by the code downloaded from http://folk.ntnu/karpa/ACER/. The possibility of clustering of up to five adjacent peaks (i.e. $k = 6$) has been considered, but the variation in the resulting Gumbel distribution is relatively small and therefore omitted in Fig. 6(b). So only the ACER result with $k = 2$ (i.e. correlation between two adjacent peaks) is included in Fig. 6(b). The ACER procedure also removes measured peaks outside an estimated confidence interval. This is the reason why the 'POT 50%, declustered' curve deviate from the '$ACER_{k=2}$' curve as de-clustering is done in the same way. The 50% threshold level chosen in the POT corresponds to the tail marker value used in ACER. Thus both results consider the same part of the tail in the peak distribution. Higher threshold levels could be chosen, but the number of peaks above the threshold then becomes smaller. The overall observation from Fig. 6(b) is that for this set of measurements a Weibull fit to the individual peak value distribution predicts a most probable largest value about 10 per cent larger than the measured maximum value. The method which here provides a most probable value closest to the measured maximum value is the POT without including possible clustering effect. Clustering seems to be important and, if included, reduces the most probable largest value to a value 5 to 15 per cent lower than the actual maximum measured value.

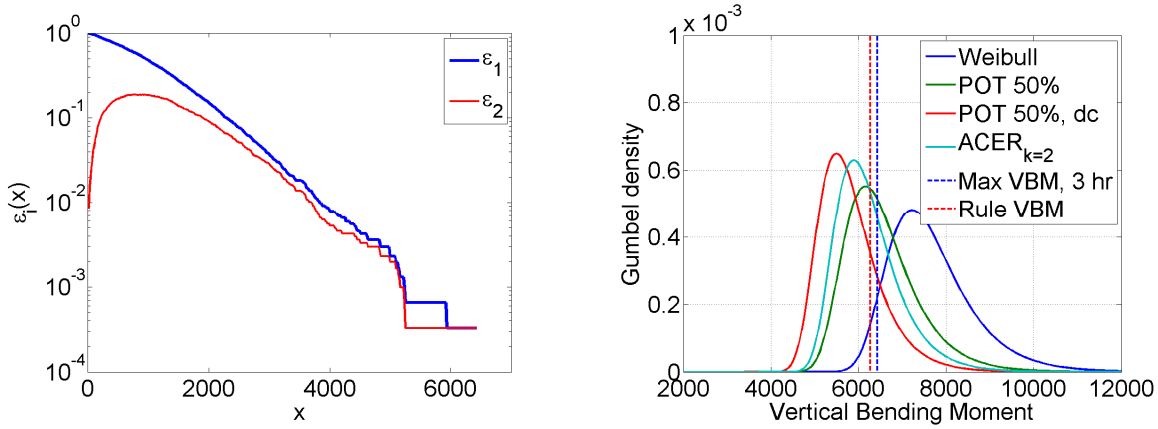

(a) Average conditional exceedance rates. (b) Gumbel distributions.

Fig. 6 Effect of de-clustering for the three hours maximum wave bending moment for the case shown in Fig.3(b). The percentage shown for the thresholds is relative to maximum measured peak value

CONCLUSIONS

The aim of the present paper has been to discuss two different procedures useful for extreme value predictions of wave-induced hydroelastic responses of marine structures.

The first procedure aims at defining proper deterministic critical wave episodes with prescribed probability content for use in very detailed and CPU demanding CFD calculations involving the complete structure and the surrounding water. The basic in the procedure is the application of the First Order Reliability Method to determine the most probable wave scenario leading to a given response. The procedure are exemplified by an analysis of the wave bending moment for the ship considered in the TULCS projects and some conclusions are given.

The second procedure deals with the analysis of full scale measurements. Here three estimation procedures are outlined for a Gumbel estimate of the extreme response: Individual peak distribution, the Peak-over-Threshold procedure and, a de-clustering procedure. The procedures are exemplified by a three hours measurement of the bending strains in the hull girder obtained in the TULCS projects and some conclusions are given.

ACKNOWLEDGEMENTS

The financial support from the EU FP7 project TULCS (Tools for Ultra Large Container Ships) project is greatly appreciated as well as the fruitful cooperation with the project partners, in particular Sime Malenica and Quentin Derbanne from Bureau Veritas, France, Jos Konig from MARIN, the Netherlands and Adolfo Maron from CEHIPAR, Spain.

REFERENCES

Der Kiureghian, A. 2000. The geometry of random vibrations and solutions by FORM and SORM. *Probabilistic Engineering Mechanics*, 15(1), pp.81-90.

Andersen, I.M.V. and Jensen, J.J., 2012. On the effect of hull girder flexibility on the vertical wave bending moment for ultra large container vessels. *Proccedings of OMAE2012,* Rio de Janeiro, Brazil, June 2012.

Andersen, I.M.V. and Jensen, J.J. 2014. Measurements in a container ship of wave-induced hull girder stresses in excess of design values. *Marine Structures*, 37, pp.54-85.

Det Norske Veritas (DNV), 2002. *Proban theory, general purpose probabilistic analysis program, Version 4.4*. Høvik: DNV.

Fujimura, K. and Der Kiureghian, A., 2007. Tail-equivalent linearization method for nonlinear random vibration. *Probabilistic Engineering Mechanics*, 22(1), pp.63-76.

Garrè L. and Der Kiureghian A., 2010. Tail-equivalent linearization method in frequency domain and application to marine structures. *Marine Structures*, 23(3), pp.322-38.

Jensen J.J. and Capul, J., 2006. Extreme response predictions for jack-up units in second order stochastic waves by FORM. *Probabilistic Engineering Mechanics*, 21(4), pp.330-337.

Jensen, J.J., 2007. Efficient estimation of extreme non-linear roll motions using the first-order reliability method (FORM). *Journal of Marine Science and Technology*, 12(4), pp.191-202.

Jensen, J.J., 2009. Stochastic procedures for extreme wave load predictions - wave bending moments in ships. *Marine Structures*, 22, pp.194-208.

Jensen, J.J., 2011. Extreme value predictions using monte carlo simulations with artificially increased load spectrum. *Probabilistic Engineering Mechanics*, 26(2), pp.399-404.

Malenica, S. and Derbanne, Q., 2012. Hydro-elastic issues in the design of ultra large container ships – TULCS project. *Proceedings of Hydroelasticity 2012*, Tokyo, 19-21 September 2012, pp 233-246.

Naess, A. and Gaidai, O., 2008. Monte carlo methods for estimating the extreme response of dynamical systems. *Journal of Engineering Mechanics, ASCE,* 134(8), pp.628-636.

Naess, A. and Gaidai, O., 2009. Estimation of extreme values from sampled time series. *Structural Safety*, 31(4), pp.325-334.

Seng, S., Jensen, J.J. and Pedersen, P.T., 2012. Numerical prediction of slamming loads. *Proceedings of IMechE, Part M: Journal of Engineering for the Maritime Environment,* 226(2), pp.120-134.

Seng, S., Andersen, I.M.V. and Jensen, J.J. 2012. On the influence of hull girder flexibility on the wave induced bending moments. *Proc. Hydroelasticity 2012, Tokyo,* 19-21 September 2012, pp 341-353

Seng, S., Jensen, J.J., 2013. An application of a free surface CFD method in the short-term extreme response analysis of ships. *Proceedings PRADS'2013*, 20-25 October 2013, CECO, Changwon City, Korea, pp.747-754

VanMarcke, E., 1975. On the distribution of the first-passage time for normal stationary random processes. *Journal of Applied Mechanics*, 42(1), pp.215-20.